IJAME

Int. J. of Applied Mechanics and Engineering, 2025, vol.30, No.2, pp.1-19
DOI: 10.59441/ijame/202710

ANALYSIS OF TRANSITIONAL STRESSES IN NON-LOCAL THERMO-ELASTIC DISC UNDER STEADY-STATE TEMPERATURE

P. Ailawalia[1*], A. Kumar[1], J. Kaur[1] and P. Jurczak[2,3]
[1]Department of Mathematics, Chandigarh University, INDIA
[2]Institute of Mechanical Engineering, University of Zielona Gora, POLAND
[3]Faculty of Technical Sciences and Economics, Collegium Witelona State University, POLAND
E-mail: praveen_2117@rediffmail.com

In solid mechanics, there are various applications of non-local theories in wave propagation, size effects, surface effects, and understanding interactions of composite materials. There are certain parameters associated with rigid bodies like stress, angular speed, and displacement which show variation with changes in temperature, thickness, density, and media. This study focuses on the evaluation of stresses, angular speed, and displacement that occur in elastic thin rotating discs. The use of local theories only investigates the effect of stress at a point that occurred due to strain at the same point. However using the non-local approach, the variation in the stresses at distant points in a material can be analyzed. This would be a significant work to understand the microstructural material characteristics. Hence this study focuses on providing a more accurate stress model for non-local thin rotating discs. The developed model for rubber, copper, and aluminum material discs is tested, to investigate the above parameters in non-local media. Further, the graphical analysis of angular speed, stresses, and displacement have been shown separately by taking thickness parameter as $k = 0$ and $k \neq 0$ in non-local media.

Key words: non-local media, rotation, disc, thickness, temperature variation, angular speed.

1. Introduction

The concept of non-local elasticity, introduced by Eringen in 1970, revolutionized classical elasticity theory by acknowledging that the stress at a given point in a material is influenced not only by the strain at that specific location but also by the strains at surrounding points. This departure from the classical local elasticity theory has far-reaching implications, particularly in materials with microstructures, defects, or heterogeneous properties, where traditional assumptions of localized interactions may not fully capture the behavior of the material [1-4]. Non-local elasticity offers a more accurate representation of stress propagation, especially in cases where distant interactions play a crucial role in the material's overall behavior.

One of the key advantages of non-local elasticity is its ability to describe lattice dispersion of elastic waves in materials with periodic structures, such as crystals. In these materials, wave propagation can be affected by interactions with the lattice, leading to phenomena like wave attenuation and dispersion. Traditional models, which assume localized interactions, fail to account for these long-range effects, whereas non-local elasticity incorporates them, offering deeper insights into wave propagation characteristics [5]. Similarly, in composite materials, where multiple phases with different mechanical properties coexist, non-local elasticity enhances the understanding of how stress and strain are transmitted across phase interfaces, which, in turn, influences the overall mechanical response and wave propagation properties of the material [6].

Beyond wave propagation, non-local elasticity also plays a significant role in the study of dislocations and fractures in materials. In crystalline materials, dislocations represent defects that disrupt the periodicity of the lattice and affect the material's mechanical properties. Non-local elasticity extends the classical theory by considering how stresses around dislocations propagate over greater distances, leading to more accurate

* To whom correspondence should be addressed

predictions of dislocation motion and crack tip stress, which is particularly valuable in materials with complex microstructures or at small length scales [3, 7]. The concept has been applied to describe phenomena in fluid interfaces, where surface tension effects are influenced by the curvature and gradient of the interface over a range of distances, offering a more comprehensive understanding of interfacial behavior [4, 6].

The applicability of non-local elasticity is particularly notable in the analysis of thermo-elastic problems, where thermal and mechanical loading interact within a material. In these problems, the behavior of materials can be significantly affected by defects, such as cracks, which modify the temperature and stress distribution. Non-local effects can play an important role in improving predictions of how thermal and mechanical fields interact, which is essential for designing materials and structures that operate under extreme conditions [2]. The study of thermo-elastic problems in solids, particularly those involving crack propagation and field distributions under thermal and mechanical loading, has long been a topic of significant interest in both theoretical and applied mechanics. Analytical approaches, such as normal mode analysis, have proven to be effective in understanding the complex interplay between thermal and elastic waves in the presence of defects like cracks [33].

A study explores the normal displacement, temperature, normal force stress, and tangential couple stress in a microstretch elastic solid subjected to a magnetic field, gravitational effects, and initial stress. The distributions of these factors are illustrated graphically. Furthermore, the paper compares the temperature, stresses, and displacements by analyzing the differences among three theories of wave propagation in a semi-infinite microstretch elastic solid under different scenarios. The classical theory of elasticity does not fully capture the behavior of many modern synthetic materials, such as elastomers and polymers, including polymethyl methacrylate (Perspex), polyethylene, and polyvinyl chloride. Instead, the linear theory of micro-polar elasticity offers a more accurate model for these materials. When considering ultrasonic waves, which involve high-frequency vibrations and small wavelengths, the microstructure of the material becomes a significant factor. This microstructural effect leads to the creation of new wave types that are not accounted for by traditional elasticity theory. Materials like metals, polymers, composites, concrete, rocks, and other solids all contain microstructures that influence their mechanical properties. Most natural and man-made materials, whether biological, geological, or engineered, exhibit microstructures that play a crucial role in determining their behavior [34].

This is particularly relevant for functionally graded materials (FGMs), which are designed to exhibit spatially varying material properties (e.g., thermal conductivity and elasticity). FGMs are increasingly used in aerospace, electronics, and energy systems due to their ability to withstand significant thermal and mechanical stresses, where traditional homogeneous materials might fail. Understanding photo-thermal-elastic interactions in FGMs is critical for optimizing their performance in real-world applications, especially under conditions of light absorption and thermal radiation, which can significantly influence the material's thermal and mechanical behavior [35].

The non-homogeneous nature of FGMs complicates their response to external thermal loads. Since material properties vary gradually across the structure, the interaction between thermal, elastic, and photo-thermal effects results in non-uniform distributions of temperature and stress. Non-local elasticity, when applied to FGMs, takes into account the long-range interactions that can modify these distributions, particularly when subjected to thermal gradients or high-intensity light irradiation. By incorporating these non-local effects, researchers have been able to explore how heat generated by external light sources or thermal loads affects the elastic response of FGMs, ensuring more accurate predictions of material performance in extreme conditions [35]. This approach also highlights the importance of controlling the non-homogeneity of the material to mitigate stress concentrations and improve the material's resilience under varying thermal and mechanical loads.

Mahdy *et al.* [36] investigated a one-dimensional problem involving a cylindrical cavity within an elastic semiconductor medium, subjected to a magnetic field and fractional heat order. The medium was modeled as linear, homogeneous, and isotropic, with initial stress. Thermal conductivity was treated as a variable, following a linear temperature dependence. The Laplace transform method was used to analyze the physical fields under a thermal ramp heating condition. The theoretical results aligned well with the physical properties of the elastic medium. Key factors such as the novel thermo-energy coupling parameter, magnetic

field, variable thermal conductivity, and fractional heat order were found to have a significant impact on the physical distributions examined. The study concluded that the normal conductivity model offers a more realistic representation compared to the fractional heat order model. Furthermore, the temperature-dependent linear variation of thermal conductivity plays a critical role in understanding the physical characteristics of semiconductor materials. Even slight changes in the models for thermal conductivity, magnetic field, and fractional heat order can result in substantial differences in the behavior of thermal-elastic-plasma wave propagation velocity.

Integrating transition theory in thermo-elastic analysis

Another important theoretical framework that has been integrated with non-local elasticity is transition theory, particularly in the study of materials subjected to load and temperature gradients. Transition theory, which focuses on finding asymptotic solutions to governing equations at critical transition points, has been used to analyze creep deformation, stress-strain behavior, and displacement components in materials ranging from isotropic to orthotropic [8-16]. This theory has been especially useful in understanding the deformation of rotating discs and other structural components where stress distributions change with rotational speed and material properties. The application of transition theory to these problems has provided valuable insights into the behavior of materials under complex thermo-mechanical loading, expanding the applicability of non-local elasticity in practical engineering problems [17].

Transition theory has also been applied to hyperbolic deformable bodies, such as radially symmetric discs under pressure, where material deformation is influenced by both internal and external forces. Studies on rotating discs, made from isotropic materials, have focused on the distribution of stress and strain, with particular attention to the transition from elastic to plastic deformation as the material undergoes increasing stress [18, 19]. Research has shown that Seth's transition theory can be applied to more general problems without requiring assumptions like yield conditions or incompressibility, which are typically needed in classical elasticity models [9, 10, 20, 21-24]. By using asymptotic solutions and generalized strain measures, this theory has facilitated the resolution of various thermo-mechanical problems and contributed to a better understanding of how materials respond to loading and thermal gradients.

The intersection of transition theory, non-local elasticity, and thermo-elastic analysis offers a powerful framework for understanding the complex behavior of materials under extreme conditions. To study the nature of stress, strain & displacement components, etc. occurring in rotating discs made of elastic, plastic, composite, or functionally graded materials, this integrated approach provides a more comprehensive view of how stress, strain, and thermal effects interact, particularly in materials with microstructures, defects, or heterogeneous properties [34]. The combination of these theories enhances our ability to design and optimize materials for high-performance applications in aerospace, electronics, and energy systems, where advanced materials must withstand a range of thermal, mechanical, and electromagnetic loading conditions.
Seth [25] defines the generalized strain measure as follows:

$$e_{ii} = \int_0^{e_{ii}^A} \left[1 - 2e_{ii}^A\right]^{\frac{n}{2}-1} de_{ii}^A = \frac{1}{n}\left[1 - \left(1 - 2e_{ii}^A\right)^{\frac{n}{2}}\right], \quad (i = 1,2,3). \tag{1.1}$$

where e_{ii}^A represents the components of Almansi finite strain, ~~and~~ 'n' denotes the measure. It yields the Cauchy, Green Hencky, Swainger, and Almansi measures for $n = -2, -1, 0, 1$, and 2, respectively.

The evaluation of stresses, angular speed, and displacement components of a rotating isotropic disc in non-local media has been done by considering the variation in thickness along the radial direction using the following relation:

$$h = h_0 \left(\frac{r}{b} \right)^{-k}. \tag{1.2}$$

Where h_0 is the thickness at $r = b$ and k is the thickness parameter. The results have been presented both graphically and quantitatively.

2. Geometrical interpretation of mathematical model

While constituting the model we consider a stiff shaft supports a thin disc that has an exterior radius of b and an interior radius of a. The disc passes through the center and spins at an ω (angular speed) perpendicular to its surface. The disc has symmetric thickness variation along the radial direction and is in a state of plane stress condition $(T_{zz} = 0)$. Here Θ is the temperature assumed at the center of the bore.

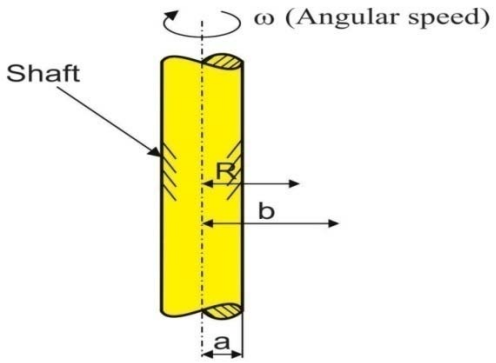

Fig.1. Mathematical model.

The disc under investigation in this study has varying thicknesses and is exposed to a field of temperature gradient. There is no external mechanical load applied on the exterior of the disc. The boundary conditions specified for the defined model are as follows:

$$\begin{aligned} T_{rr} &= 0 \quad \text{at} \quad r = b, \\ u &= 0 \quad \text{at} \quad r = a, \end{aligned} \tag{2.1}$$

where u denotes the displacement component and T_{rr} denotes stress in a radial direction.

3. Problem statement

By using the cylindrical polar coordinates, Seth [25] has provided the displacement components:

$$u = r(1-\beta), \quad v = 0, \quad w = dz. \tag{3.1}$$

Where $\beta = f(r), \left(r = \sqrt{x^2 + y^2} \right)$ only and d is a constant.

The components of strain are described using cylinder polar coordinates [25, 26]:

$$e_{rr}^{A} \equiv \frac{\partial u}{\partial r} - \frac{1}{2}\left(\frac{\partial u}{\partial r}\right)^2 = \frac{1}{2}\left[1 - \left(r\beta' + \beta\right)^2\right],$$

$$e_{zz}^{A} \equiv \frac{\partial w}{\partial z} - \frac{1}{2}\left(\frac{\partial w}{\partial z}\right)^2 = \frac{1}{2}\left[1 - (1-d)^2\right],$$

$$e_{r\theta}^{A} = e_{\theta z}^{A} = e_{zr}^{A} = 0, \tag{3.2}$$

$$e_{\theta\theta}^{A} \equiv \frac{u}{r} - \frac{u^2}{2r^2} = \frac{1}{2}\left[1 - \beta^2\right],$$

where $\beta' = \dfrac{d\beta}{dr}$ and the superscript A indicates that it refers to the Almansi strain.

Substituting the values of strain components from equation (3.2) in (1.1) the components of strain in a generalized form are described as:

$$e_{rr} = \frac{1}{n}\left[1 - \left(r\beta' + \beta\right)^n\right],$$

$$e_{\theta\theta} = \frac{1}{n}\left[1 - \beta^n\right], \tag{3.3}$$

$$e_{zz} = \frac{1}{n}\left[1 - \left(1-d\right)^n\right],$$

and

$$e_{r\theta}^{A} = e_{\theta z}^{A} = e_{zr}^{A} = 0,$$

For thermo-elastic isotropic materials, the stress-strain relationship is provided by [27]:

$$T_{ij} = \lambda\delta_{ij} I_1 + 2\mu e_{ij} - \xi\Theta\delta_{ij}, \left(i, j = 1,2,3\right). \tag{3.4}$$

Where $I_1 = e_{kk}$ is the first strain invariant, $\xi = \alpha\left(3\lambda + 2\mu\right)$, and Θ is the temperature. Further, Θ has to satisfy [25]

$$\nabla^2\Theta = 0, \qquad \frac{d^2\Theta}{dr^2} + \frac{1}{r}\frac{d^2\Theta}{dr^2} \equiv \frac{1}{r}\frac{d}{dr}\left(r\frac{d\Theta}{dr}\right) = 0 \qquad \text{or} \qquad \frac{d\Theta}{dr} = \frac{A_1}{r}.$$

Which has the solution

$$\Theta = A_1\left(\log r + A_2\right). \tag{3.5}$$

where A_1 and A_2 are constants of integration and can determined from the boundary condition.

The temperature that satisfies relation (3.5), along with the boundary conditions, can be determined as follows:

$$\Theta = \Theta_0, \text{ at } \quad r = a,$$

$$\Theta = 0, \quad \text{at} \quad r = b,$$

where Θ_0 is constant.
Use boundary conditions to obtain A_1 and A_2 :

$$A_1 = \frac{\Theta}{\log \frac{a}{b}} \quad \text{and} \quad A_2 = -\log b \, .$$

Substituting A_1 and A_2 in relation (3.5), we get:

$$\Theta = \frac{\Theta_0 \log \frac{r}{b}}{\log \frac{a}{b}} .$$

Equation (3.4) for this problem becomes:

$$T_{rr} = \frac{2\lambda\mu}{(\lambda + 2\mu)}[e_{rr} + e_{\theta\theta}] + 2\mu e_{rr} - \frac{2\mu\xi\Theta}{(\lambda + 2\mu)},$$

$$T_{\theta\theta} = \frac{2\lambda\mu}{(\lambda + 2\mu)}[e_{rr} + e_{\theta\theta}] + 2\mu e_{\theta\theta} - \frac{2\mu\xi\Theta}{(\lambda + 2\mu)}, \tag{3.6}$$

$$T_{r\theta} = T_{\theta z} = T_{zr} = T_{zz} = 0.$$

The strain components derived in terms of stresses are as follows:

$$e_{rr} = \frac{\partial u}{\partial r} - \frac{1}{2}\left(\frac{\partial u}{\partial r}\right)^2 = \frac{1}{2}\left[1 - (r\beta' + \beta)^2\right] = \frac{1}{E}\left[T_{rr} - \left(\frac{1 - C}{2 - C}\right)T_{\theta\theta}\right] + \alpha\Theta,$$

$$e_{zz} = \frac{\partial w}{\partial z} - \frac{1}{2}\left(\frac{\partial w}{\partial z}\right)^2 = \frac{1}{2}\left[1 - (1 - d)^2\right] = -\frac{(1 - C)}{E(2 - C)}[T_{rr} + T_{\theta\theta}] + \alpha\Theta,$$

(3.7)

$$e_{r\theta} = e_{\theta z} = e_{zr} = 0,$$

$$e_{\theta\theta} = \frac{u}{r} - \frac{u^2}{2r^2} = \frac{1}{2}\left[1 - \beta^2\right] = \frac{1}{E}\left[T_{\theta\theta} - \left(\frac{1 - C}{2 - C}\right)T_{rr}\right] + \alpha\Theta,$$

where E and C expressed in terms of Lames constants, as $E=\frac{\mu(3\lambda+2\mu)}{(\lambda+\mu)}$ and $C=\frac{2\mu}{(\lambda+2\mu)}$, $\alpha=\frac{C\xi}{E(2-C)}$.

Substituting the strain components given by equation (3.3) in (3.6), we get:

$$\tau_{rr}=\frac{2\mu}{n\left(1-\zeta^2\nabla^2\right)}\left[3-2C-\beta^n\left\{1-C-(2-C)(1+P)^n+\frac{nC\xi\Theta}{2\mu\beta^n}\right\}\right],$$

$$T_{r\theta}=T_{\theta z}=T_{zr}=T_{zz}=0, \tag{3.8}$$

$$\tau_{\theta\theta}=\frac{2\mu}{n\left(1-\zeta^2\nabla^2\right)}\left[3-2C-\beta^n\left\{2-C-(1-C)(1+P)^n+\frac{nC\xi\Theta}{2\mu\beta^n}\right\}\right].$$

Using the value of local stress tensor in terms of non-local stress tensor [28]

$$T_{ij}=\left(1-\zeta^2\nabla^2\right)\tau_{ij}.$$

All equilibrium equations are met except for [26]:

$$\frac{d}{dr}(rhT_{rr})-hT_{\theta\theta}+\rho\omega^2r^2h=0. \tag{3.9}$$

Where ρ represents the density of the material of the rotating disc.

Use equation (3.8) in (3.9), to obtain a non-linear differential equation in β as:

$$(2-C)n\beta^{(n+1)}P(P+1)^{n-1}\frac{dP}{d\beta}=\frac{nrh'}{2\mu h}\left(1-\zeta^2\nabla^2\right)\tau_{rr}+\frac{n\rho\omega^2r^2}{2\mu}-\frac{nC\xi\Theta_0}{2\mu}, \tag{3.10}$$

where $\bar{\Theta}_0=\Theta_0/\log\frac{a}{b}$ and $r\beta'=\beta P$ [20-25] and β depends on r.

4. Identification of the solution

To determine the transition stresses in a rotating disc, define the transition function (φ) (see Seths and Hulsurkar [10, 11, 12, 25, 29], Gupta [9, 21, 22], Thakur [23, 24, 30]) at the critical point (transition point) that is $P\to\pm\infty$, for the elastic state.

$$\varphi=\frac{n}{2\mu}[T_{\theta\theta}-C\xi\Theta]=\left[(3-2C)-\beta^n\left\{2-C+(1-C)(1+P)^n\right\}-\frac{nC\xi\Theta}{\mu}\right], \tag{4.1}$$

$$\frac{d(\log\varphi)}{dr}=-\frac{nP\beta^n}{r}\left[\frac{2-C+(1-C)(1+P)^{n-1}\left\{1+P+\beta\frac{dP}{d\beta}\right\}}{3-2C-\beta^n\left\{2-C+(1-C)(1+P)^n\right\}-\frac{nC\xi\Theta}{\mu}}\right]. \tag{4.2}$$

After substituting the value of $\frac{dP}{d\beta}$ from equation (3.10) in (4.2) and considering $P \to \pm\infty$ and then integrating, we obtained:

$$\varphi = \frac{B_1 r^{v-1}}{h}, \tag{4.3}$$

where $v = \frac{1-C}{2-C}$ and B_1 is a constant of integration.
Using the value of h from equation (1.2) in (4.1) and subsequently in equation (4.2), we have

$$\tau_{\theta\theta} = \frac{2\mu}{n\left(1-\zeta^2\nabla^2\right)} \cdot \frac{B_1 r^{v+k+1} b^{-k}}{h_0} + \frac{C\xi\Theta_0 \log\frac{r}{b}}{\left(1-\zeta^2\nabla^2\right)\log\frac{a}{b}}. \tag{4.4}$$

Substituting the value of φ given by equation (4.3) in (3.9) using relation and then integrating, we get

$$\begin{aligned}\tau_{rr} = {} & \frac{2\mu}{nv\left(1-\zeta^2\nabla^2\right)} \cdot \frac{B_1 r^{v+k+1} b^{-k}}{h_0} - \frac{\rho\omega^2 r^2}{(3-k)\left(1-\zeta^2\nabla^2\right)} + \frac{B_2 b^{-k}}{h_0 r^{1-k}\left(1-\nabla^2\zeta^2\right)} + \\ & + \frac{C\xi\Theta_0 \log\frac{r}{b}}{\left(1-\zeta^2\nabla^2\right)\log\frac{a}{b}} - \frac{C\xi\Theta_0}{\left(1-\zeta^2\nabla^2\right)\log\frac{a}{b}}.\end{aligned} \tag{4.5}$$

Where, B_2 is the constant of integration.
Substituting the values from equations (4.3) and (4.4) in the second equation of relation (3.7), we get:

$$\beta = \sqrt{1 - \frac{2v\left(1-\zeta^2\nabla^2\right)}{E}\left[\frac{\rho\omega^2 r^2}{3-k} - \frac{B_2 b^{-k}}{h_0 r^{1-k}} + \frac{\alpha E\Theta_0 (2-C)}{\log\frac{a}{b}} + \frac{2(2-C)\alpha E\Theta_0 \log\frac{r}{b}}{(1-C)\log\frac{a}{b}}\right]}, \tag{4.6}$$

where $C\xi = \alpha E(2-C)$.
Again, substituting the value of τ_{rr} from equations (4.5) in equation (3.1), we obtain:

$$u = r - r\sqrt{1 - \frac{2v\left(1-\zeta^2\nabla^2\right)}{E}\left[\frac{\rho\omega^2 r^2}{3-k} - \frac{B_2 b^{-k}}{h_0 r^{1-k}} + \frac{\alpha E\Theta_0 (2-C)}{\log\frac{a}{b}} + \frac{2(2-C)\alpha E\Theta_0 \log\frac{r}{b}}{(1-C)\log\frac{a}{b}}\right]}. \tag{4.7}$$

The Young's modulus in terms of compressibility factor is defined as $E = \frac{2\mu(3-2C)}{(2-C)}$. Using the relations (4.4) and (4.6) in the boundary conditions given by (2.1) we obtain,

$$B_1 = \frac{\rho\omega^2 nvh_0 b^k \left(b^{3-k} - a^{3-k}\right)}{2\mu(3-k)b^v} + \frac{\alpha E\Theta_0 nv(2-C)(b-a)}{2\mu\log\frac{a}{b}\, b^{\frac{(1-C)}{(2-C)}}} - \frac{\alpha E\Theta_0 na}{\mu b^{\frac{(1-C)}{(2-C)}}}, \tag{4.8}$$

$$B_2 = \frac{\rho\omega^2 a^{3-k} h_0}{(3-k)b^{-k}} + \frac{\alpha E\Theta_0 (2-C)a}{\log\left(\frac{a}{b}\right)} + \frac{2(2-C)\alpha E\Theta_0 a}{(1-C)}. \tag{4.9}$$

Using relations (4.7) and (4.8) in equations (4.3), (4.4), and (4.6) respectively, we get:

$$\tau_{\theta\theta} = \frac{\rho\omega^2 vr^k \left(b^{3-k} - a^{3-k}\right)}{\left(1-\zeta^2\nabla^2\right)(3-k)r}\left(\frac{r}{b}\right)^v + \\ + \frac{\alpha E\Theta_0 (2-C)}{\left(1-\zeta^2\nabla^2\right)}\left[\frac{\log\frac{r}{b}}{\log\frac{a}{b}} - \frac{2a}{(2-C)r}\left(\frac{r}{b}\right)^{\frac{(1-C)}{(2-C)}} + \frac{(1-C)(b-a)}{r(2-C)\log\frac{a}{b}}\left(\frac{r}{b}\right)^{\frac{(1-C)}{(2-C)}}\right], \tag{4.10}$$

$$\tau_{rr} = \frac{\rho\omega^2 r^2}{r(3-k)\left(1-\zeta^2\nabla^2\right)}\left[\left(b^{3-k} - a^{3-k}\right)\left(\frac{r}{b}\right)^v - r^{3-k} + a^{3-k}\right] + \frac{\alpha E\Theta_0 (2-C)}{\left(1-\zeta^2\nabla^2\right)\log\frac{a}{b}} \times \\ \times\left[\log\frac{r}{b} + \frac{a}{r} - 1 + \frac{(b-a)}{r}\left(\frac{r}{b}\right)^{\frac{(1-C)}{(2-C)}}\right] + \frac{2\alpha E\Theta_0 (2-C)}{(1-C)\left(1-\zeta^2\nabla^2\right)}\left[\frac{a}{r} - \frac{a}{r}\left(\frac{r}{b}\right)^{\frac{1-C}{2-C}}\right], \tag{4.11}$$

$$u = r - r\left\{1 - \frac{2v\left(1-\zeta^2\nabla^2\right)}{E}\left[\frac{\rho\omega^2\left(r^{3-k} - a^{3-k}\right)}{(3-k)r^{1-k}} + \frac{\alpha E\Theta_0 (2-C)(r-a)}{r\log\frac{a}{b}} + \right.\right. \\ \left.\left. + \frac{2(2-C)\alpha E\Theta_0}{(1-C)}\left[\frac{\log\frac{r}{b}}{\log\frac{a}{b}} - \frac{a}{r}\right]\right]\right\}^{\frac{1}{2}} \tag{4.12}$$

and

$$\left|\tau_{rr} - \tau_{\theta\theta}\right| = \frac{\rho\omega^2 r^k}{r(3-k)\left(1-\zeta^2\nabla^2\right)}\left[(1-v)\left(b^{3-k} - a^{3-k}\right)\left(\frac{r}{b}\right)^v - r^{3-k} + a^{3-k}\right] + \\ + \frac{\alpha E\Theta_0}{\left(1-\zeta^2\nabla^2\right)}\left[2\left(\frac{a}{r}\right)\left(\frac{2-C}{1-C}\right) - \frac{2}{(1-C)r}\left(\frac{r}{b}\right)^{\frac{1-C}{2-C}} + \frac{(b-a)}{r\log\frac{a}{b}}\left(\frac{r}{b}\right)^{\frac{1-C}{2-C}} + \frac{(2-C)(a-r)}{r\log\frac{a}{b}}\right]. \tag{4.13}$$

From equation (4.13), it is evident that $\left|\tau_{rr}-\tau_{\theta\theta}\right|$ [10, 25, 29] is highest at the inner surface (at $r=a$) which results in yielding to take place at its inner surface. Further, equation (4.13) can be represented by the following relation:

$$\left|\tau_{rr}-\tau_{\theta\theta}\right|_{r=a}=\frac{\rho\omega^2\left(b^{3-k}-a^{3-k}\right)}{(3-k)\left(1-\zeta^2\nabla^2\right)a^{1-k}}\left(\frac{a}{b}\right)^{v}+$$
$$+\left[\frac{\alpha E\Theta_0}{\left(1-\nabla^2\zeta^2\right)}\right]\left[\frac{(b-a)}{a\log\frac{a}{b}}\left(\frac{a}{b}\right)^{\left(\frac{1-C}{2-C}\right)}+\frac{2(2-C)}{1-C}-\frac{2}{1-C}\left(\frac{a}{b}\right)^{\nu}\right]\equiv Y(say). \tag{4.14}$$

The angular speed required for initial yielding is expressed as [21-23]:

$$\Omega_i^2=\frac{\rho\omega_i^2b^2}{Y},$$

$$\Omega_i^2=\left|\frac{\left(1-\nabla^2\zeta^2\right)(3-k)ab^2}{(1-v)\left(b^{3-k}-a^{3-k}\right)a^k}\left(\frac{b}{a}\right)^{v}\right|-$$
$$+\frac{3(2-C)(\alpha E\Theta_0)}{Y\left(1-\left(\frac{a}{b}\right)^3\right)}\left[\frac{1-\frac{a}{b}}{log\frac{a}{b}}-\frac{2a}{b(1-C)}+\frac{2(2-C)}{1-C}\left(\frac{a}{b}\right)^{\frac{1}{2-C}}\right]. \tag{4.15}$$

and

$$\omega_i=\frac{\Omega_i}{b}\sqrt{\frac{Y}{\rho}},$$

where,

$$\rho\omega_i^2=\frac{(3-k)aY\left(1-\zeta^2\nabla^2\right)}{(1-v)a^k\left(b^{3-k}-a^{3-k}\right)}\left(\frac{b}{a}\right)^{v}-$$
$$+\frac{(3-k)a\alpha E\Theta_0}{(1-v)a^k\left(b^{3-k}-a^{3-k}\right)}\left(\frac{b}{a}\right)^{v}\left\{\frac{b-a}{a\log\frac{a}{b}}\left(\frac{a}{b}\right)^{v}+\frac{2(2-C)}{1-C}-\frac{2}{1-C}\left(\frac{a}{b}\right)^{v}\right\}.$$

Take $(C\to 0)$ in equation (4.13) the value of stress difference in a fully plastic state is given as follows:

$$\left|\tau_{rr}-\tau_{\theta\theta}\right|_{r=b}=\left|\frac{\rho\omega^2\left(b^{3-k}-a^{3-k}\right)}{2(3-k)\left(1-\zeta^2\nabla^2\right)b^{1-k}}+\frac{\alpha E\Theta_0}{\left(1-\zeta^2\nabla^2\right)}\left[\frac{(b-a)}{b\log\frac{a}{b}}-2\left(\frac{a}{b}\right)\right]\right|=Y^*(say).$$

Further, Ω required for the same state is given by [21-23]:

$$\Omega_f^2 = \frac{\rho\omega_f^2 b^2}{Y^*},$$

$$\Omega_f^2 = \left|\frac{2\left(1-\nabla^2\zeta^2\right)(3-k)b^{3-k}}{\left(b^{3-k}-a^{3-k}\right)}\right| - \left|\frac{6\alpha E\Theta_0}{\left(1-\left(\frac{a}{b}\right)^3\right)Y^*}\left[\frac{1-\frac{a}{b}}{log\frac{a}{b}}-\frac{2a}{b}\right]\right|, \tag{4.16}$$

where

$$\omega_f = \frac{\Omega_f}{b}\sqrt{\frac{Y^*}{\rho}} \qquad \text{and} \qquad \rho\omega_f^2 = \frac{2(3-k)b^{3-k}}{\left(b^{3-k}-a^{3-k}\right)}\left[\left(1-\zeta^2\nabla^2\right)Y^* - \alpha E\Theta_0\left\{\frac{b-a}{b\log\frac{a}{b}}-\frac{2a}{b}\right\}\right].$$

We are introducing the above components in non-dimensional form:

$$\varphi = \frac{r}{b},\quad \varphi_0 = \frac{a}{b},\quad \sigma_{rr} = \frac{\tau_{rr}}{Y},\quad \sigma_{\theta\theta} = \frac{\tau_{\theta\theta}}{Y},\quad U = \frac{u}{b},\quad \Theta_1 = \frac{E\alpha\Theta_0}{Y},\quad \Omega^2 = \frac{\rho\omega^2 b^2}{Y},\quad H = \frac{Y}{E}.$$

Components of transition stresses, Ω and U from equation (4.10), (4.11), (4.15), and (4.12) in non-dimensional form become:

$$\sigma_{\theta\theta} = \left(\frac{\Omega_i^2 v\left(1-\varphi_0^{3-k}\right)\varphi^{v+k-1}}{(3-k)\left(1-\zeta^2\nabla^2\right)}\right) + \frac{(2-C)\Theta_1}{\left(1-\zeta^2\nabla^2\right)}\left[\frac{(1-C)(1-\varphi_0)\varphi^{\frac{-1}{2-C}}}{(2-C)\log\varphi_0} + \frac{\log\varphi}{\log\varphi_0} - \frac{2\varphi_0}{2-C}\varphi^{\frac{-1}{2-C}}\right], \tag{4.17}$$

$$\begin{aligned}\sigma_{rr} = {} & \frac{\Omega_i^2\varphi^{k-1}}{(3-k)\left(1-\zeta^2\nabla^2\right)}\left[\left(1-\varphi_0^{3-k}\right)\varphi^v - \varphi^{3-k} + \varphi_0^{3-k}\right] + \\ & + \frac{2(2-C)\Theta_1}{(1-C)\left(1-\zeta^2\nabla^2\right)}\left[\frac{\varphi_0}{R} - \frac{\varphi_0}{\varphi}\varphi^{\frac{1-C}{2-C}}\right] + \frac{(2-C)\Theta_1}{\left(1-\zeta^2\nabla^2\right)\log\varphi_0}\left[\log\varphi + \frac{\varphi_0}{\varphi} - 1 + \frac{(1-\varphi_0)}{\varphi}\varphi^{\frac{1-C}{2-C}}\right],\end{aligned} \tag{4.18}$$

$$\Omega_i^2 = \left|\frac{(3-k)\left(1-\zeta^2\nabla^2\right)\varphi_0^{1-v-k}}{(1-v)\left(1-\varphi_0^{3-k}\right)}\right| - \left|\frac{3(2-C)\Theta_1}{1-\varphi_0^3}\left[\frac{1-\varphi_0}{\log\varphi_0} + \frac{2(2-C)}{1-C}\varphi_0^{\frac{1}{2-C}} - \frac{2}{1-C}\varphi_0\right]\right|, \tag{4.19}$$

$$\Omega_i^2 = \frac{\rho\omega^2 b^2}{Y},$$

and

$$U=\varphi-\varphi\Bigg\{1-2\nu H\left(1-\zeta^2\nabla^2\right)\Bigg[\frac{\Omega_i^2\varphi^{k-1}\left(\varphi^{3-k}-\varphi_0^{3-k}\right)}{(3-k)}+ \\ +\frac{(2-C)(\varphi-\varphi_0)\Theta_1}{\varphi\log\varphi_0}+\frac{2(2-C)\Theta_1}{(1-C)}\left\{\frac{\log\varphi}{\log\varphi_0}-\frac{\varphi_0}{\varphi}\right\}\Bigg]\Bigg\}^{\frac{1}{2}}. \tag{4.20}$$

The expressions for Ω, $\sigma_{\theta\theta}$, σ_{rr} and U for the fully plastic state $(C\to 0)$, are obtained from equations(4.16), (4.17), (4.18) and (4.20) respectively as follows:

$$\sigma_{\theta\theta}=\frac{\Omega_f^2\left(1-\varphi_0^{3-k}\right)\varphi^k}{2(3-k)\sqrt{\varphi}\left(1-\zeta^2\nabla^2\right)}+\frac{2\Theta_1}{\left(1-\zeta^2\nabla^2\right)}\left\{\frac{\log\varphi}{\log\varphi_0}+\frac{1-\varphi_0}{2\sqrt{\varphi}\log\varphi_0}-\frac{\varphi_0}{\sqrt{\varphi}}\right\}, \tag{4.21}$$

$$\sigma_{rr}=\frac{\Omega_f^2\varphi^{k-1}}{(3-k)\left(1-\zeta^2\nabla^2\right)}\left[\left(1-\varphi_0^{3-k}\right)\sqrt{\varphi}-\varphi^{3-k}+\varphi_0^{3-k}\right]+ \\ +\frac{4\Theta_1}{\left(1-\zeta^2\nabla^2\right)}\left\{\frac{\varphi_0}{\varphi}-\frac{\varphi_0}{\sqrt{\varphi}}\right\}+\frac{2\Theta_1}{\left(1-\zeta^2\nabla^2\right)\log\varphi_0}\left\{\log\varphi-1+\frac{\varphi_0}{\varphi}+\frac{1-\varphi_0}{\sqrt{\varphi}}\right\}, \tag{4.22}$$

$$U=\varphi-\varphi\Bigg\{1-H\left(1-\zeta^2\nabla^2\right)\Bigg[\frac{\Omega_f^2\varphi^{k-1}\left(\varphi^{3-k}-\varphi_0^{3-k}\right)}{3-k}+ \\ +\frac{2\Theta_1(\varphi-\varphi_0)}{\varphi\log\varphi_0}+4\Theta_1\left(\frac{\log\varphi}{\log\varphi_0}-\frac{\varphi_0}{\varphi}\right)\Bigg]\Bigg\}^{\frac{1}{2}}, \tag{4.23}$$

$$\Omega_f^2=\left|\frac{2(3-k)\left(1-\zeta^2\nabla^2\right)}{1-\varphi_0^{3-k}}\right|-\left|\frac{6\Theta_1}{1-\varphi_0^3}\left\{\frac{1-\varphi_0}{\log\varphi_0}-2\varphi_0\right\}\right|, \tag{4.24}$$

At $\zeta\neq 0$, the transitional stresses given by equations (4.17)-(4.20) (taking $C\neq 0$) become

$$\sigma_{\theta\theta}=\left(\frac{\Omega_i^2\nu\left(1-\varphi_0^{3-k}\right)\varphi^{\nu+k-1}}{(3-k)\left(1-\zeta^2\nabla^2\right)}\right)+\frac{(2-C)\Theta_1}{\left(1-\zeta^2\nabla^2\right)}\left[\frac{(1-C)(1-\varphi_0)\varphi^{\frac{-1}{2-C}}}{(2-C)\log\varphi_0}+\frac{\log\varphi}{\log\varphi_0}-\frac{2\varphi_0}{2-C}\varphi^{\frac{-1}{2-C}}\right], \tag{4.25}$$

$$\sigma_{rr}=\frac{\Omega_i^2\varphi^{k-1}}{(3-k)\left(1-\zeta^2\nabla^2\right)}\left[\left(1-\varphi_0^{3-k}\right)\varphi^{\nu}-\varphi^{3-k}+\varphi_0^{3-k}\right]+ \\ +\frac{2(2-C)\Theta_1}{(1-C)\left(1-\zeta^2\nabla^2\right)}\left[\frac{\varphi_0}{\varphi}-\frac{\varphi_0}{\varphi}\varphi^{\frac{1-C}{2-C}}\right]+\frac{(2-C)\Theta_1}{\left(1-\zeta^2\nabla^2\right)\log\varphi_0}\left[\log\varphi+\frac{\varphi_0}{\varphi}-1+\frac{(1-\varphi_0)}{\varphi}\varphi^{\frac{1-C}{2-C}}\right], \tag{4.26}$$

$$\Omega_i^2 = \left| \frac{(3-k)\left(1-\nabla^2\zeta^2\right)\varphi_0^{1-v-k}}{(1-v)\left(1-\varphi_0^{3-k}\right)} \right| - \left| \frac{3(2-C)\Theta_1}{1-\varphi_0^3} \left[\frac{1-\varphi_0}{log\varphi_0} + \frac{2(2-C)}{1-C}\varphi_0^{\frac{1}{2-C}} - \frac{2\varphi_0}{1-C} \right] \right|, \tag{4.27}$$

$$U = \varphi - \varphi\left\{1 - 2vH\left(1-\zeta^2\nabla^2\right)\left[\frac{\Omega_i^2\varphi^{k-1}\left(\varphi^{3-k}-\varphi_0^{3-k}\right)}{(3-k)} + \right.\right.$$
$$\left.\left. + \frac{(2-C)(\varphi-\varphi_0)\Theta_1}{\varphi\log\varphi_0} + \frac{2(2-C)\Theta_1}{(1-C)}\left\{ \frac{\log\varphi}{\log\varphi_0} - \frac{\varphi_0}{\varphi} \right\} \right] \right\}^{\frac{1}{2}}. \tag{4.28}$$

5. Particular case

At $\zeta = 0$ and $C \neq 0$, the transitional stresses given by equation (4.17) reduce to:

$$\sigma_{\theta\theta} = \left(\frac{\Omega_i^2 v\left(1-\varphi_0^{3-k}\right)\varphi^{v+k-1}}{(3-k)} \right) + (2-C)\Theta_1 \left[\frac{(1-C)(1-\varphi_0)\varphi^{\frac{-1}{2-C}}}{(2-C)\log\varphi_0} + \frac{\log\varphi}{\log\varphi_0} - \frac{2\varphi_0}{2-C}\varphi^{\frac{-1}{2-C}} \right], \tag{5.1}$$

$$\sigma_{rr} = \frac{\Omega_i^2\varphi^{k-1}}{(3-k)}\left[\left(1-\varphi_0^{3-k}\right)\varphi^v - \varphi^{3-k} + \varphi_0^{3-k} \right] + \frac{2(2-C)\Theta_1}{(1-C)}\left[\frac{\varphi_0}{\varphi} - \frac{\varphi_0}{\varphi}\varphi^{\frac{1-C}{2-C}} \right] +$$
$$+ \frac{(2-C)\Theta_1}{\log\varphi_0}\left[\log\varphi + \frac{\varphi_0}{\varphi} - 1 + \frac{(1-\varphi_0)}{\varphi}\varphi^{\frac{1-C}{2-C}} \right], \tag{5.2}$$

$$\Omega_i^2 = \left| \frac{(3-k)\varphi_0^{1-v-k}}{(1-v)\left(1-\varphi_0^{3-k}\right)} \right| - \left| \frac{3(2-C)\Theta_1}{1-\varphi_0^3} \left[\frac{1-\varphi_0}{\log\varphi_0} + \frac{2(2-C)}{1-C}\varphi_0^{\frac{1}{2-C}} - \frac{2}{1-C}\varphi_0 \right] \right|, \tag{5.3}$$

$$U = \varphi - \varphi\left\{1 - 2vH\left[\frac{\Omega_i^2\varphi^{k-1}\left(\varphi^{3-k}-\varphi_0^{3-k}\right)}{(3-k)} + \frac{(2-C)(\varphi-\varphi_0)\Theta_1}{\varphi\log\varphi_0} + \right.\right.$$
$$\left.\left. + \frac{2(2-C)\Theta_1}{(1-C)}\left\{ \frac{\log\varphi}{\log\varphi_0} - \frac{\varphi_0}{\varphi} \right\} \right] \right\}^{\frac{1}{2}}, \tag{5.4}$$

$\sigma_{\theta\theta}$, σ_{rr}, U and Ω for the fully plastic state (when $\to 0$) are derived from the relations given by (4.21)-(4.24) as:

$$\sigma_{\theta\theta} = \frac{\Omega_f^2\left(1-\varphi_0^{3-k}\right)\varphi^k}{2(3-k)\sqrt{\varphi}} + 2\Theta_1\left\{ \frac{\log\varphi}{\log\varphi_0} + \frac{1-\varphi_0}{2\sqrt{\varphi}\log\varphi_0} - \frac{\varphi_0}{\sqrt{\varphi}} \right\}, \tag{5.5}$$

$$\sigma_{rr}=\frac{\Omega_f^2\varphi^{k-1}}{(3-k)}\left[\left(1-\varphi_0^{3-k}\right)\sqrt{\varphi}-\varphi^{3-k}+\varphi_0^{3-k}\right]+4\Theta_1\left\{\frac{\varphi_0}{\varphi}-\frac{\varphi_0}{\sqrt{\varphi}}\right\}+$$
$$+\frac{2\Theta_1}{\log\varphi_0}\left\{\log\varphi-1+\frac{\varphi_0}{\varphi}+\frac{1-\varphi_0}{\sqrt{\varphi}}\right\}, \tag{5.6}$$

$$\Omega_f^2=\left|\frac{2(3-k)}{1-\varphi_0^{3-k}}\right|-\left|\frac{6\Theta_1}{1-\varphi_0^3}\left\{\frac{1-\varphi_0}{\log\varphi_0}-2\varphi_0\right\}\right|, \tag{5.7}$$

$$U=\varphi-\varphi\sqrt{1-H\left[\frac{\Omega_f^2\varphi^{k-1}\left(\varphi^{3-k}-\varphi_0^{3-k}\right)}{3-k}+\frac{2\Theta_1(\varphi-\varphi_0)}{\varphi\log\varphi_0}+4\Theta_1\left\{\frac{\log\varphi}{\log\varphi_0}-\frac{\varphi_0}{\varphi}\right\}\right]}. \tag{5.8}$$

6. Numerical illustration and discussion

For the analysis of angular velocity, stress, and displacement, consider the following parameters; Poisson's ratio $(\nu)=0.33$ for aluminum, *0.428* for gold, *0.33* for copper, *0.5* for rubber, compressibility factor C is $0.00, 0.25, 0.5$, ratio $\frac{E}{Y}=0.5$ and *2*, initial temperature $\Theta_0=0F$ and $700F$, thermal expansion coefficient $\alpha=5\times10^{-5}F$ (for methyl methacrylate). Parameter $\Theta_1=\frac{\alpha E\Theta_0}{Y}$, resulting in values $0, 0.0125, 0.25$ for $H=\frac{E}{Y}=0.5,2$ and $\Theta_0=0F$, $700F$ respectively [15, 31, 32]. Curves in Figures 2 and 3 represent the comparison of initial yielding angular speed Ω_i^2 and fully plastic angular speed Ω_f^2 w.r.t radii ratios $\nu=0.5, 0.333, 0.428$, at $k=0, 1$ different temperature values $(\Theta_1=0, 0.0125, 0.25)$ for both local and non-local media respectively.

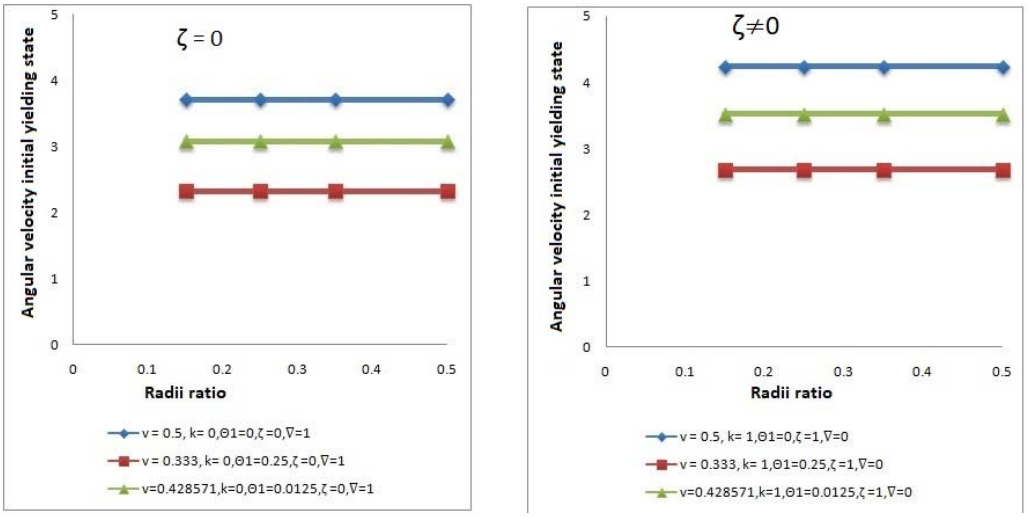

Fig.2. Angular velocity (Ω) vs radii ratio (R) in initial yielding $(k=0,1)$.

From Fig.2, it can be seen that, in the presence of thickness parameter i.e. $k=1$, a rotating disc made of non-compressible material(rubber) required maximum angular velocity to yield at the inner surface of the disc as compared to those made of compressible materials (copper, gold, and aluminum) in the non-local media, which leads to the safer design. However, Fig.3, reveals the reverse pattern in the case of angular velocity in the fully plastic state. Moreover, in the absence of the thickness parameter, $k=0$, both have the same values in local and non-local media. Figure 4, shows the variation of circumferential stresses $\sigma_{\theta\theta}$ with radii ratio. It can be seen that circumferential stresses are high at the outer surface of the disc in non-local media for $k=0,1$ under temperature conditions for compressible and non-compressible material. However, from Fig.5, it can be seen that, radial stresses are high at the internal surface of the disc under temperature variation for non-local media for both $k=0, 1$, with minimum value of radial stresses at the outer surface of the disc for local and non-local media. Fig. 6, shows the comparison of displacement and radius of both the media under temperature and thickness variation. The displacement is negligible at the internal surface. This result is valid for every value of ζ or ∇ except $\zeta=1$ and $\nabla=1$.

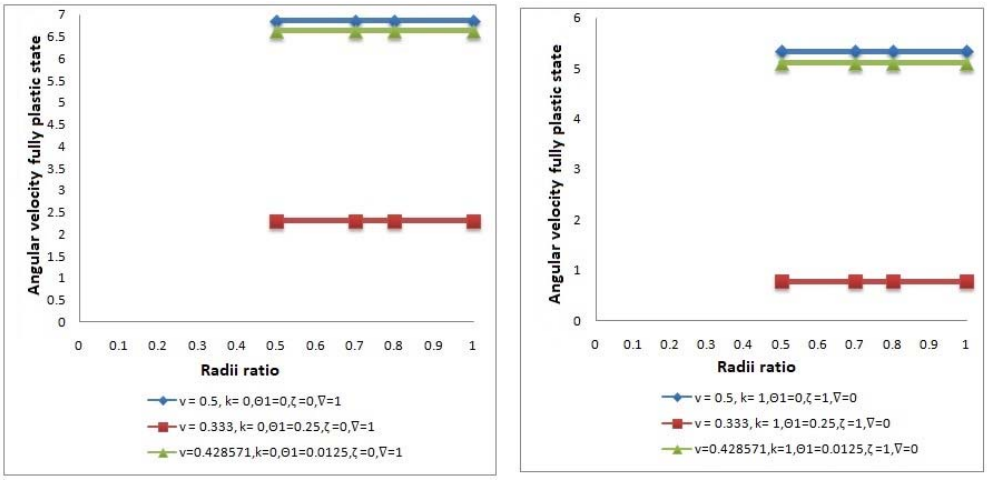

Fig.3. Angular velocity (Ω) vs radii ratio (R) in the fully plastic state $(k=0,1)$.

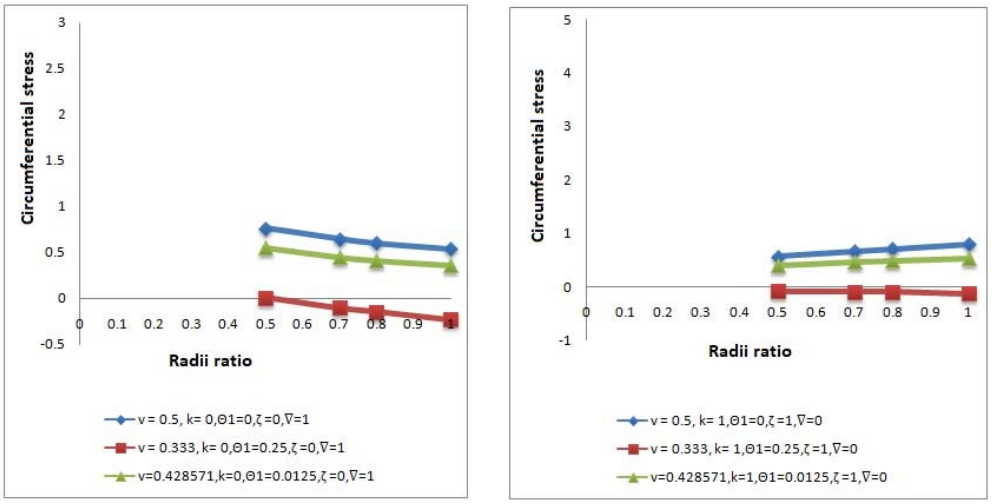

Fig.4. Stress (circumferential $\sigma_{\theta\theta}$) vs. radii ratio $R(k=0,1)$.

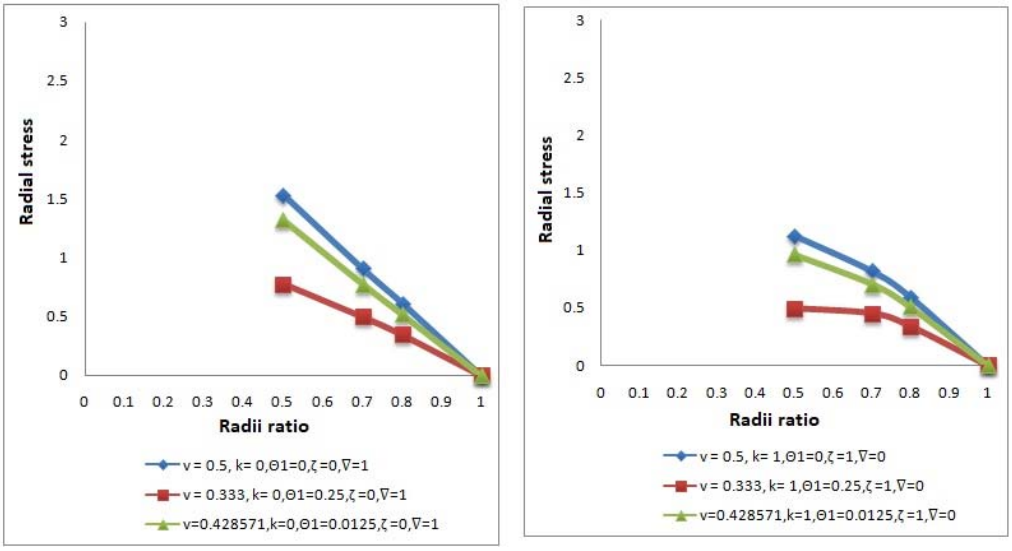

Fig.5. Stress (radial σ_{rr}) vs radii ratio $R(k=0,1)$.

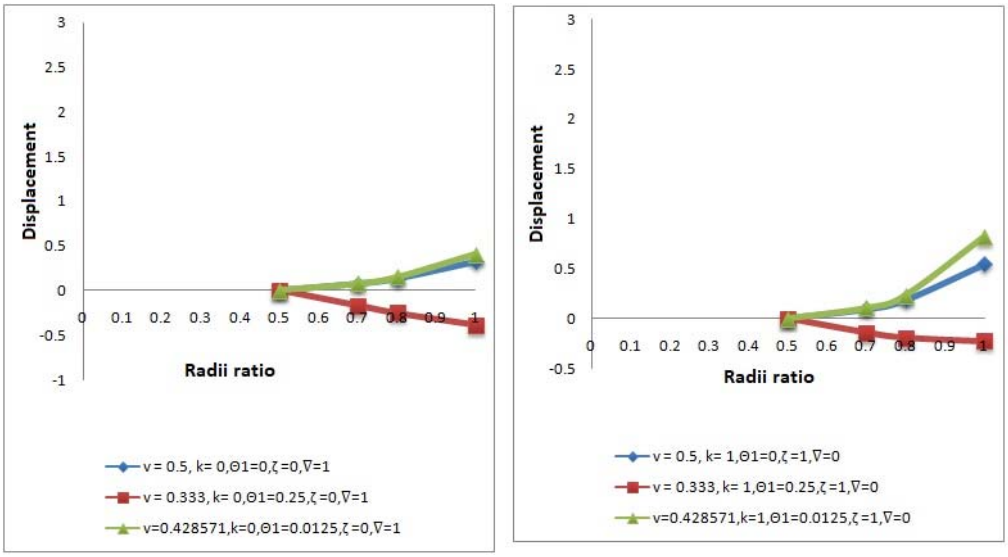

Fig.6. Displacement u vs. Radii ratio $R(k=0,1)$.

7. Conclusion

The results are calculated for both local and non-local media in the absence and presence of thickness parameter k, and it can be seen that rotating discs made of non-compressible materials like rubber require a higher value of angular velocity to yield at the inner surface compared to those made of compressible materials like copper and aluminum. As the radii ratio increases, Ω also increases. However, thickness variation results in lesser value of Ω to deform at the inner surface as compared to non-compressible material for local and non-local media. Thermal effects have also reduced the value of angular speed, however, results reverse when variations in thickness take place. It is also analyzed that radial stress σ_{rr} for non-compressible material has shown a maximum value at the inner surface as compared to compressible material in non-local media, while the value of radial stress in local media is higher as compared to non-local media. The displacement of

compressible material with an increase in radius ratio towards the external radii as compared to non-compressible material for both media.

Nomenclature

A_1, A_2 – constants of integration
B_1, B_2 – constants of integration
b, a – disc's external and internal radii
C – compressibility
k – thickness parameter
r, z, θ – radial, axial and circumferential direction
T_{ij}, e_{ij} – stress and strain rate tensor
u, w, v – displacement components
Y – yield stress
α – coefficient of thermal expansion
δ_{ij} – Kronecker's delta function
Θ – temperature
Θ_1 – $(\alpha E \Theta_0)/Y$ or Y^*
ν – Poisson ratio
ρ – density of material
σ_{rr} – radial stress component (τ_{rr}/Y)
$\sigma_{\theta\theta}$ – circumferential stress component $(\tau_{\theta\theta}/Y)$,
τ_{ij} – non-local stress tensor
ζ – parameter of non-local media
Ω^2 – $\dfrac{\rho\omega^2 b^2}{Y}$ (speed factor); $\varphi = r/b$ and $\varphi_0 = a/b$
ω – angular velocity of rotation

References

[1] Eringen A.C. (1977): *Screw dislocation in non-local elasticity*.– Journal of Physics D: Applied Physics, vol.10, No.5, pp.671-678.

[2] Dhaliwal J.W.R.S. (1993): *Uniqueness in generalized nonlocal thermoelasticity*.– Journal of Thermal Stresses, vol.16, No.1, pp.71-77.

[3] Eringen A.C., Speziale C. and Kim B. (1977): *Crack-tip problem in non-local elasticity*.– Journal of the Mechanics and Physics of Solids, vol.25, No.5, pp.339-355.

[4] Peddieson J., Buchanan G.R. and McNitt R.P.(2003): *Application of nonlocal continuum models to nanotechnology*.– International Journal of Engineering Science, vol.41, No.3-5, pp.305-312.

[5] Sharma V., Ailawalia P. and Kumar S. (2024): *Wave propagation in a hygrothermoelastic half-space along with non-local variable*.– Journal of Applied Science and Engineering, vol.27, No.5, pp.2445-2452.

[6] Reddy J. (2007): *Nonlocal theories for bending, buckling and vibration of beams*.– International Journal of Engineering Science, vol.45, No.2-8, pp.288-307.

[7] Lu P., Lee H., Lu C. and Zhang P. (2006): *Dynamic properties of flexural beams using a nonlocal elasticity model*.– Journal of Applied Physics, vol.99, No.7, pp.073510-073519.

[8] Thakur P. and Sethi M. (2020): *Creep deformation and stress analysis in a transversely material disk subjected to rigid shaft*.– Mathematics and Mechanics of Solids, vol.25, No.1, pp.17-25.

[9] Gupta S. and Thakur P. (2008): *Creep transition in an isotropic disc having variable thickness subjected to internal pressure*.– Proceedings of The National Academy of Sciences India Section A-Physical Sciences, vol.78, pp.57-56.

[10] Seth B. (1962): *Transition theory of elastic-plastic deformation, creep and relaxation*.– Nature, vol.195, No.4844, pp.896-897.

[11] Seth B. (1970): *Transition conditions: the yield condition*.– International Journal of Non-Linear Mechanics, vol.5, No.2, pp.279-285.

[12] Hulsurkar S. (1966): *Transition theory of creep of shells under uniform pressure*.– ZAMM-Journal of Applied Mathematics and Mechanics, vol.46, No.7, pp.431-437.

[13] Temesgen A., Singh S. and Thakur P. (2020): *Modeling of creep deformation of a transversely isotropic rotating disc with a shaft having variable density and subjected to a thermal gradient*.– Thermal Science and Engineering Progress, vol.20, pp.1-24.

[14] Shahi S., Singh S. B. and Thakur P. (2019): *Modeling creep parameter in rotating discs with rigid shaft exhibiting transversely isotropic and isotropic material behavior*.– Journal of Emerging Technologies and Innovative Research, vol.6, No.1, pp.387-395.

[15] Thakur P. and Sethi M. (2020): *Elastoplastic deformation in an orthotropic spherical shell subjected to a temperature gradient*.– Mathematics and Mechanics of Solids, vol.25, No.1, pp.26-34.

[16] Sethi M. and Thakur P. (2020): *Elastoplastic deformation in an isotropic material disk with shaft subjected to load and variable density*.– Journal of Rubber Research, vol.23, No.2, pp.69-78.

[17] Narmarta S., Kaur J., Thakur P. and Murali G. (2023): *Structural behaviour of annular isotropic disk made of steel/copper material with gradually varying thickness subjected to internal pressure*.– Structural Integrity and Life, vol.23, p.293297.

[18] Heyman J. (1958): *Plastic design of rotating discs*.– Proceedings of the Institution of Mechanical Engineers, vol.172, No.1, pp.531-547.

[19] Chakrabarty J. and Drugan W. (1998): *Theory of Plasticity*.– Journal of Applied Mechanics, 1988.

[20] Gupta S. and Shukla R. (1994): *Elastic-plastic transition in a thin rotating disc*.– Ganita, vol.45, No.2, pp.79-85.

[21] Gupta S. (2007): *Creep transition in a thin rotating disc with rigid inclusion*.– Defence Science Journal, vol.57, No.2, pp.185-195.

[22] Gupta K. S. (2007): *Thermo elastic-plastic transition in a thin rotating disc with inclusion*.– Thermal Science, vol.11, No.1, pp.103-118.

[23] Thakur P. (2011): *Elastic-plastic transition stresses in a disc having variable thickness and poissons ratio subjected to internal pressure*.– International Journal of Mathematics and Computer Applications Research (IJMCAR), No.31, pp.51-73.

[24] Thakur P., Singh S. and Kaur J. (2013): *Thickness variation parameter in a thin rotating disc by finite deformation*.– FME Transactions, vol.41, No.2, pp.96-102.

[25] Seth B. (1966): *Measure-concept in mechanics*.– International Journal of Non-Linear Mechanics, vol.1, No.1, pp.35-40.

[26] Sokolnikoff I. (1948): *On the use of conformal mapping in two-dimensional problems of the theory of elasticity*.– Applied Mathematics Series, No.18, pp.71-77.

[27] Parkus H. (2012): *Thermoelasticity*.– Springer Science Business Media.

[28] Abouelregal A.E. (2022): *Response of thermoelastic cylindrical cavity in a non-local infinite medium due to a varying heat source*.– Waves in Random and Complex Media, vol.32, No.4, pp.1725-1742.

[29] Seth B. (1963): *Elastic-plastic transition in shells and tubes under pressure*.– ZAMM-Journal of Applied Mathematics and Mechanics, vol.43, No.7-8, pp.345-351.

[30] Thakur P. (2013): *Effect of stresses in a thin rotating disk with edge load for different materials*.– Advanced Technologies and Materials, vol.38, No.1, pp.43-55.

[31] Thakur P., Sethi M., Gupta N. and Gupta K. (2021): *Thermal effects in rectangular plate made of rubber, copper and glass materials*.– Journal of Rubber Research, vol.24, pp.147-155.

[32] Hahn D.W. and Özisik M.N. (2012): *Heat conduction*.– John Wiley & Sons.

[33] Lotfy K. (2012): *Mode-I crack in a two-dimensional fibre-reinforced generalized thermoelastic problem*.– Chinese Physics B, vol.21, No.1, p.014209.

[34] Othman M.I., Abo-Dahab S.M. and Lotfy K. (2014): *Gravitational effect and initial stress on generalized magneto-thermo-microstretch elastic solid for different theories*.– Applied Mathematics and Computation, vol.230, pp.597-615.

[35] Lotfy K. and Tantawi R.S. (2020): *Photo-thermal-elastic interaction in a functionally graded material (FGM) and magnetic field*.– Silicon, vol.12, No.2, pp.295-303.

[36] Mahdy A.M., Lotfy K. and El-Bary A.A. (2022): *Use of optimal control in studying the dynamical behaviors of fractional financial awareness models*.– Soft Computing, vol.26, No.7, pp.3401-3409.

Received: August 29, 2024
Revised: March 7, 2025